

## Numerical results

The experimental results obtained by dimensional analysis and dielectric measurements are used as input data for the simulation of the transport phenomena inside a realistic DEP device for nanoparticle trapping from flue gas. First we compute the pDEP force distribution inside a typical DEP device and then we move to the problem of determining the distribution profile of nanoparticles under the influence of dielectrophoresis. Finally, we analyze and discuss the obtained numerical results in terms of *Filtration rate*, a global quantity correlated with the concentration field, which offers a more suggestive characterization of the capabilities of the device regarding the separation process of nanoparticles from flue gas. All the numerical simulations were performed using the *COMSOL Multiphysics* program.

For the computation of the pDEP force, we first solved the Laplace equation for the real and imaginary components of the electric potential, together with the associated boundary conditions. The computational domain consists of a unit cell described by the following set of geometric parameters:  $d=l=100\ \mu\text{m}$ ,  $H=500\ \mu\text{m}$  and  $w=2\ \mu\text{m}$ . The simulations were performed for a suspension of particles with characteristic sizes  $a=50\text{nm}$ ,  $a=100\text{nm}$  and  $a=200\text{nm}$  respectively, in air. The dielectric response of the particles is characterized by the real part of the CM factor  $K_R=1$  and we considered the amplitude of the electric potential applied on the electrodes in the range  $V_0=12\div 24\text{V}$ . The macroscopic behavior of a suspension of spherical particles of radius  $a$  in a fluid of viscosity  $\eta$  is modeled by considering the mechanical equilibrium between an external force  $\mathbf{F}$  (DEP force in this case) and the Stokes drag force. For small particles (i.e. nanoparticles), the dynamics of the system is governed by the following system of equations:

$$\mathbf{v} = \mathbf{u} + \frac{2a^2}{9\eta} \mathbf{F}, \quad (1a)$$

$$\frac{\partial C}{\partial t} + \nabla \cdot \mathbf{j} = 0, \quad \text{where } \mathbf{j} = C\mathbf{v} - D\nabla C. \quad (1b)$$

Here  $\mathbf{u}$  and  $\mathbf{v}$  are the fluid and particle velocities,  $t$  is the time,  $\mathbf{j}$  is the particle flux,  $D$  is the diffusion coefficient of the particles, and  $C$  is the particle volume concentration.

The fluid flow field inside the separation device,  $\mathbf{u}$ , is calculated by solving the classical Navier-Stokes equation in the compressible case, together with the corresponding boundary conditions. For the obtained DEP-force and fluid flow field, the particle concentration is evaluated by numerically integrating equations (1a) and (1b). This calculated particle concentration field gives information at a local scale, showing how the particles are attracted on the margins of electrodes and the influence of the main parameters of the problem on this process. For the analysis of the filtration process we define the novel quantity named *Filtration rate* ( $F$ ), which describes the process in terms of nanoparticles entrapment at the electrodes, related to the concentration distribution:

$$F = \frac{C_{input} - C_{output}}{C_{input}} = 1 - C_{output}/C_{input} \quad [\%] \quad (2)$$

where  $C_{input}$  and  $C_{output}$  are the mean concentrations of suspended nanoparticles at the input and the output surfaces of the device, respectively, as schematically sketched in Figure 1.

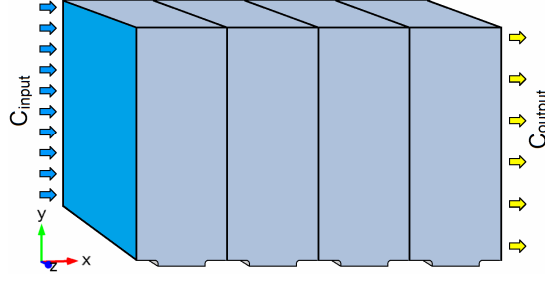


Figure 1: Schematic representation of the separation device revealing the parameters used for defining the *Filtration rate*.

This proposed quantity gives the global information on the filtration process, and can be used in order to evaluate the efficiency of the filtration process.

At the end of this theoretical section is important to conclude that the electrokinetic forces depend in a complex manner on system dimensions, frequency, field, etc. In separation systems, the buoyancy force can be sometimes significant (as in FFF) but often the magnitude of this force is much lower than the other forces acting on nanoparticles.

In order to avoid numerical difficulties, due mainly to the extremely wide range of variation of the DEP force inside the computational domain, we chose to solve the model equations in the dimensionless form. If the electric potential is scaled with the applied electrode voltage  $V_0$ , the distances with the electrode width  $d$ , the time with  $d^2 / D$ , the velocities with  $D / d$ , and the particle volume fraction with the initial average volume fraction  $C_0$ , the corresponding dimensionless form of the DEP force (1) is:

$$\langle \mathbf{F}_{DEP} \rangle = F_{0DEP} \nabla' \left( |\nabla' V_R'|^2 + |\nabla' V_I'|^2 \right). \quad (3)$$

We noted in the above equation  $F_{0DEP} = 2\pi a^3 \epsilon_m K_R (V_0^2 / d^3)$  a quantity that measures the intensity of the external field. The prime symbol above denotes the dimensionless quantities.

The magnitude of the vector  $\nabla' \left( |\nabla' V_R'|^2 + |\nabla' V_I'|^2 \right)$ , proportional to the dimensionless DEP force given by (3), calculated in the vicinity of the electrodes, is presented in Figure 2a) in logarithmic scale. The results clearly show that the pDEP force reaches its maximum near the electrodes' margins (a difference of at least two orders of magnitude), and diminishes rapidly with the height. Practically, at heights  $y > d$  the dielectrophoretic effect is negligible. The nanoparticles subjected to the calculated pDEP force are strongly attracted to the electrodes edges, while their volume concentration in fluid diminishes, as showed in Figure 2b).

The efficiency of the filtration process can be evaluated by calculating the *Filtration rate* (2) for different values of problem's parameters. The computation is performed using an iterative procedure: the output concentration in one unit cell is considered the input concentration for the next unit cell, in order to describe the cumulative effect of the filtration inside the dielectrophoretic device. This type of analysis allows an estimation of the necessary number of cells (or electrodes) in order to obtain a certain desired filtration rate, when the other parameters of the problem are fixed. The results presented in Figure 3a) show that in the case of particle having size of 100nm, a desired filtration rate of 90% can be obtain by using about 30 electrodes when applying a voltage of 24 V, about 60 electrodes for 18 V, and nearly 200 electrodes for an applied voltage of 12 V.

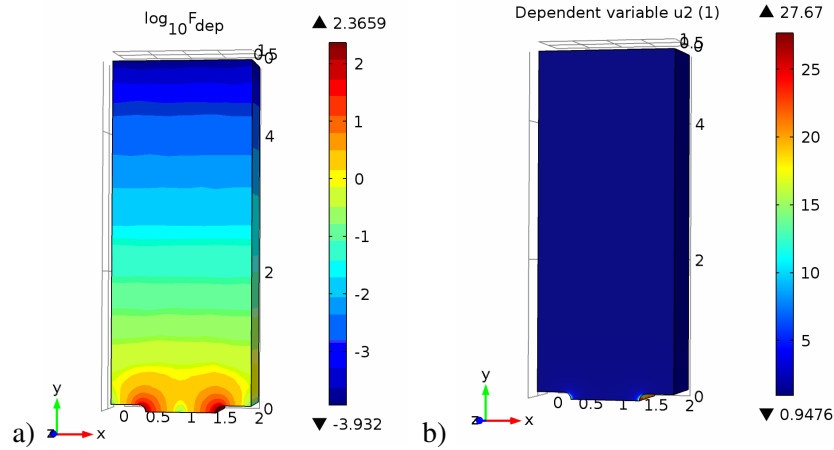


Figure 2: The magnitude of the vector  $\nabla'(|\nabla'V_R|^2 + |\nabla'V_I|^2)$ , in logarithmic scale, a) and calculated particle concentration distribution for a typical separation device, b).

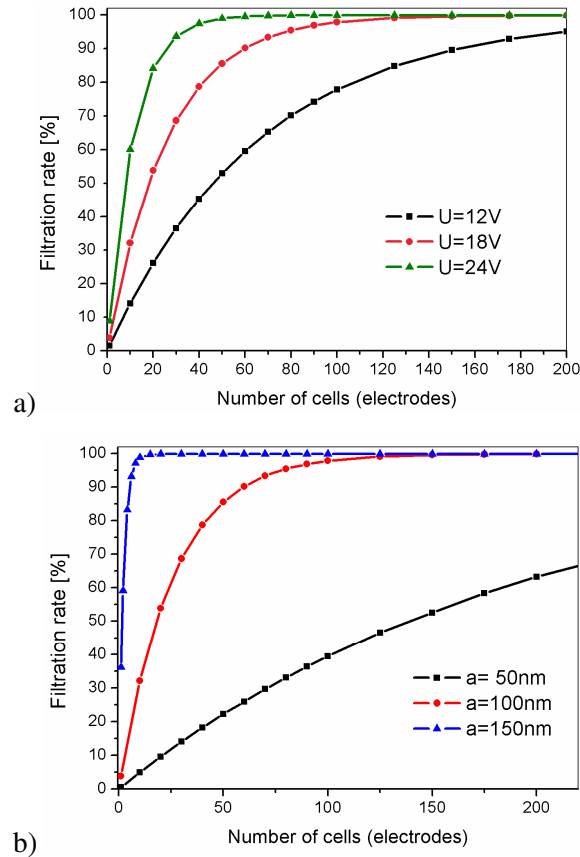


Figure 3: Calculated filtration rate versus number of cells for a) particles with  $a=100\text{nm}$  at three different applied voltages and b) particles with three different radii at an fixed applied voltage of  $V_0 = 18\text{V}$  ( $d = l = 100\ \mu\text{m}$ ,  $w = 2\ \mu\text{m}$ ).

When we analyze the effect of particle radii on the filtration capacity, the results presented in Figure 3b) predict that, for example, when the applied voltage is 18 V, particles of 150 nm are completely captured after 10 electrodes, for particles of 100 nm we need about 150 electrodes for

the complete capture, while for the particles of 50 nm are captured less than 60% even if one use devices with 250 electrodes.

In conclusion, the simulations performed in the frame of the presented mathematical model allow an estimation of the performances of the filtration as a function of the geometric and physical parameters of the problem. The next step of our research activity focused on the validation of the proposed model is presented in section *Experimental device and results*.